Country	Subject Area and Category	Publisher
SCIMAGO INSTITUTIONS RANKINGS SCImago Media Rankings	Engineering └ Engineering (miscellaneous) Physics and Astronomy └ Physics and Astronomy (miscellaneous)	Japan Society of Applied Physics

SJR 2024	H-Index
0.427 Q2	115

Publication type	ISSN	Coverage
Journals	18820778, 18820786	2008-2025

Editorial Board

JOURNAL LINKS

Submit an article

About the journal

Editorial Board

Author guidelines

Publication charges

News and editorial

Awards

Journal collections

Pricing and ordering

Contact us

Japanese Journal of Applied Physics

IOPSCIENCE

Journals

Books

IOP Conference Series

About IOPscience

Contact Us

Developing countries access

IOP Publishing open access policy

Accessibility

IOP PUBLISHING

Terms and Conditions

Disclaimer

Privacy and Cookie Policy

Text and Data mining policy

PUBLISHING SUPPORT

Authors

Reviewers

Conference Organisers

Reproducible perovskite solar cells using a simple solvent-mediated sol–gel synthesized NiOx hole transport layer

by Ersan Y. Muslih

Applied Physics Express 15, 015504 (2022) LETTER
https://doi.org/10.35848/1882-0786/ac435d

Reproducible perovskite solar cells using a simple solvent-mediated sol–gel synthesized NiO_x hole transport layer

Ersan Y. Muslih[1,2], Md. Shahiduzzaman[3*], Md. Akhtaruzzaman[4*], Mohammad Ismail Hossain[5], LiangLe Wang[6], Hend I. Alkhammash[7], Sami S. Alharthi[8], Masahiro Nakano[1], Makoto Karakawa[1,3], Mohammod Aminuzzaman[9,10], Lai-Hock Tey[9], Kamaruzzaman Sopian[4], Jean-Michel Nunzi[3], and Tetsuya Taima[1,3,6*]

[1]Graduate School of Natural Science and Technology, Kanazawa University, Kakuma, Kanazawa 920–1292, Japan
[2]Mechanical Engineering Department, Faculty of Industrial Technology, Trisakti University, Jakarta 11440, Indonesia
[3]Nanomaterials Research Institute, Kanazawa University, Kakuma, Kanazawa 920–1192, Japan
[4]Solar Energy Research Institute (SERI), Universiti Kebangsaan Malaysia (UKM), 43600 Bangi, Selangor, Malaysia
[5]Department of Electrical and Computer Engineering, University of California, Davis, 1 Shields Avenue, Davis, CA 95616, United States of America
[6]Graduate School of Frontier Science Initiative, Kanazawa University, Kakuma, Kanazawa 920–1192, Japan
[7]Department of Electrical Engineering, College of Engineering, Taif University, P.O.Box 11099, Taif 21944, Saudi Arabia
[8]Department of Physics, College of Science, Taif University, PO Box 11099, Taif 21944, Saudi Arabia
[9]Department of Chemical Science, Faculty of Science, Universiti Tunku Abdul Rahman, Perak Campus, Jalan Universiti, Bandar Barat, 31900 Kampar, Perak D. R., Malaysia
[10]Centre for Photonics and Advanced Materials Research (CPAMR), Universiti Tunku Abdul Rahman, Jalan Sungai Long, Bandar Sungai Long, 43000 Kajang, Selangor, Malaysia

*E-mail: shahiduzzaman@se.kanazawa-u.ac.jp; akhtar@ukm.edu.my; taima@se.kanazawa-u.ac.jp

Received November 29, 2021; revised December 8, 2021; accepted December 14, 2021; published online January 6, 2022

A nickel oxide (NiO_x) hole transport layer was made from nickel oxide powder by a simple process and non-stabilizer or chelating agent. We used ethanol as the main solvent and less than 2% nitric acid as the co-solvent. The formation reaction mechanism of the NiO_x thin film was also studied. Perovskite solar cells (PSCs) with an optimum thickness of 70 nm exhibited a power conversion efficiency as high as 12.99%, which is superior to those of PSCs with their counterparts. The moisture stability of NiO_x-based devices (non-encapsulated) remained above 70% of their initial output after 700 h storage at ambient conditions.

Supplementary material for this article is available online

Since being discovered by Park in 2012,[1)] organic–inorganic halide perovskite solar cells (PSCs) have triggered rapid development and much attention because of their potential to more developed relatively low-cost processing, up-scale applicable, and having two well-known conventional n-i-p and inverted p-i-n structures.[2–4)] Both structure-based devices use organic materials such as 2,2′,7,7′-tetrakis[N,N-di(4-methoxyphenyl)amino]-9,9′-spirobifluorene (spiro-OMeTAD) and polymer poly[bis(4-phenyl)(2,4,6-trimethylphenyl)amine] (PTAA) as the hole transport layers (HTLs), which are high-cost and low-stability.[5,6)] Thus, inorganic HTL materials attract more attention to replace the organic HTLs due to superior hole-mobility and outstanding stability. Inorganic p-type semiconductor materials such as CuI, CuSCN, and NiO_x have been developed as HTL in PSCs to solve these problems.[7–11)] Among inorganic HTL, nickel oxide (NiO_x) is the most prominent and attractive HTLs mentioned above because it is relatively inert and intrinsically p-type with a wide bandgap (3.15–4.3 eV).[9–14)] Typically, NiO_x thin film is made by sol-gel from nickel salts such as nickel acetate, nickel nitrate, and nickel acetylacetonate.[9,15–21)] However, those sol-gel techniques are time-consuming and require a stabilizer or complexing agents such as ethanolamine that can have high sheet resistance, resistivity, low conductivity, and low carrier concentration.[21–24)] Previously, Akhtaruzzaman and colleagues[25)] produced NiO_x powder particles with a diameter of 100 nm or bigger by green synthesis. In terms of PSC application, these bigger NiO_x particles cannot be a suitable candidate as the solely HTL because inadequate surface coverage and electron blockage leads to perovskite penetration into FTO-substrate and makes a short circuit. Therefore, it is important to make NiO_x particles as a compact and dense thin film for HTL application in PSCs, which has not been studied in-depth and used as an HTL solely for PSCs applications.

In this work, a compact NiO_x thin film has been successfully synthesized from nickel oxide powder using a simple solution mixture between low content nitric acid as a co-solvent and ethanol as the main solvent and applied as the HTL for inverted PSCs. The inverted p-i-n structure-based device was chosen due to relatively low process temperature and is widely open to making a tandem solar cell with conventional low-bandgap p-type photovoltaics.[26–29)] The reaction mechanism of the formation NiO_x thin film was also investigated. NiO_x thin films showed a favorable energy level with perovskite film, most importantly low-cost and environment-friendly synthesis capabilities. The HTL exhibits a high crystallinity, suitable optical properties, good performance, and good stability of inverted PSCs.

Metal oxides are immiscible in water or other solvents with similar to water properties such as alcohol. Thus, to solve NiO_x powder, nitric acid was added and followed with heat treatment at 85° for about 10 min. This treatment can ionize the NiO_x into Ni^{2+} and react with NO_3^- and water molecules to form complex compounds that dissolve in ethanol. Besides being the main solvent, ethanol also reduces surface tension so that the solution can stick to the substrate more. Figure 1 shows the few steps of the NiO_x thin-film making process from NiO_x powder. In the solving process, the reaction would only happen if assisted by heating and made an azeotrope compound with nitrate and water molecules. This process was marked by color changing from a black powder into a green solution. NiO_x powder was dissolved in nitric acid and water molecules to make some ionic complex compounds. At this point, the nickel complex molecule was surrounded by

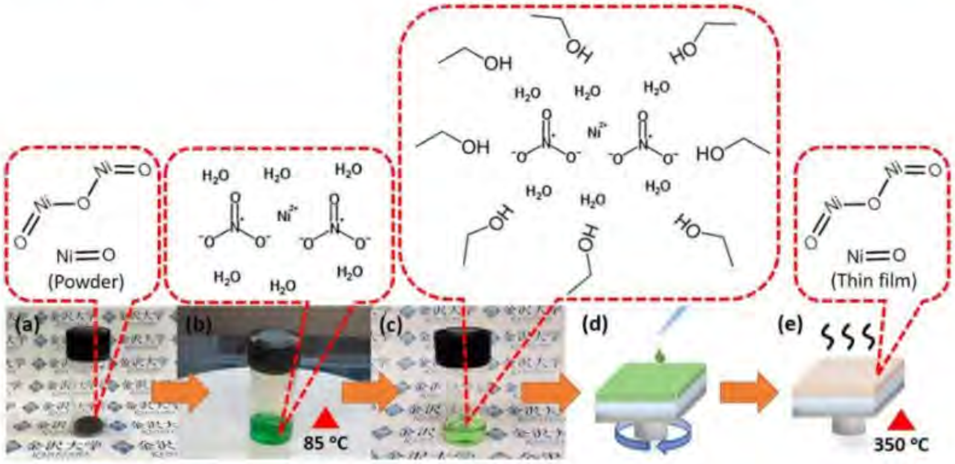

Fig. 1. (Color online) (a) NiO_x powder (b) NiO_x powder dissolving process with nitric acid and heat, (c) appearance of NiO_x solution after diluted with ethanol, (d) illustration of NiO_x solution deposited on FTO glass by spin-coating, (e) annealing illustration of NiO_x thin film.

ethanol molecules as its solvent. Besides solvation interaction, there is also hydrogen bonding between water and ethanol.[30] This phenomenon was easily recognized when the color was changed and easily dissolved in ethanol and recorded by a UV–vis spectrophotometry peak shift from 394 nm to 399 nm, as shown in Fig. 2(a). Furthermore, this solution was deposited on FTO and followed by annealing to obtain NiO_x thin films. Finally, nickel ion underwent an oxidation reaction or condensation and formed NiO_x. These reactions were matched with Boetcher et al.,[31] which explains the reactions of metal-oxide synthesis from metal-nitrate in detail. However, the reactions in this research were divided into three stages, the first is the dissolution reaction, the second is the nitrate thermal decomposition, and the last stage is the metal oxide formation stage. Overall, the NiO_x thin film synthesis was described as using the following reactions:

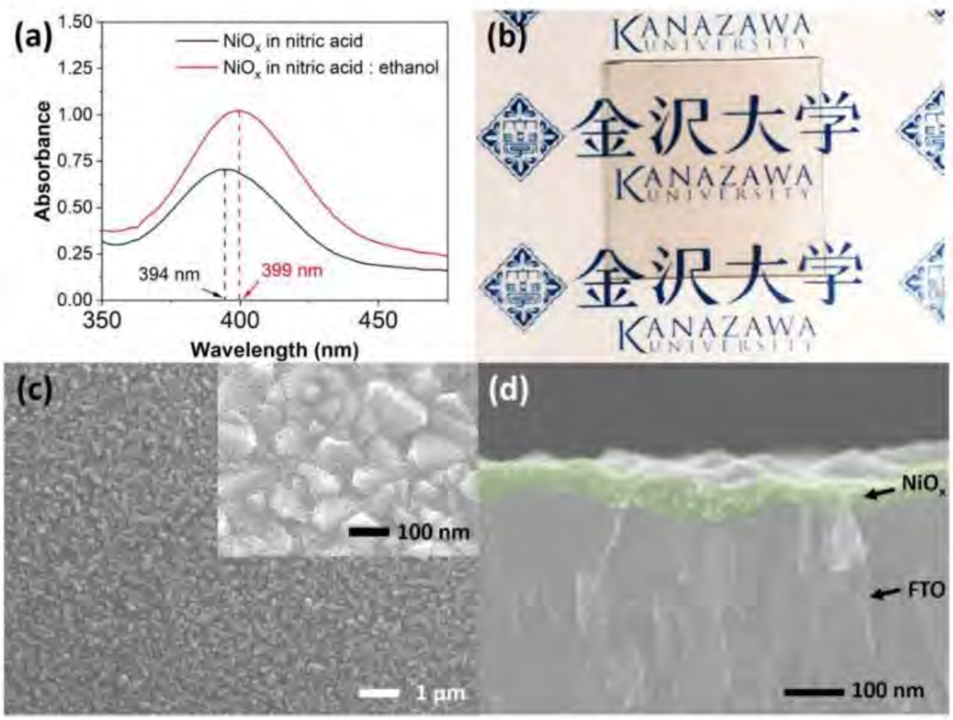

Fig. 2. (Color online) (a) The UV–vis spectra for NiO_x in nitric acid and nitric acid with ethanol, (b) NiO_x thin film appearance after annealing, (c) top view SEM image of NiO_x thin film, and (d) cross-sectional SEM image of NiO_x thin film on FTO.

Dissolution Reaction:

$$NiO_x(s) + 2\,HNO_3\,(aq) + Z\,H_2O(aq) \rightarrow Ni(NO_3)_x.ZH_2O\,(aq) \quad (1)$$

$$Ni(NO_3)_x.ZH_2O\,(aq) \rightarrow [Ni(H_2O)_z]^{x+}(aq) + Z\,HNO_3(aq) \quad (2)$$

Nitrate Thermal Decomposition:

$$Ni(NO_3)_x.ZH_2O\,(aq) \rightarrow Ni(OH)_x(aq) + X\,NO_2(g) + Z\,H_2O\,(g) \quad (3)$$

$$4\,HNO_3(aq) \rightarrow 4\,NO_2(g) + O_2(g) + 2\,H_2O\,(g) \quad (4)$$

Metal Oxide Formation:

$$Ni(OH)_x(aq) \rightarrow NiO_x(s) + Z\,H_2O\,(g) \quad (5)$$

$$[Ni(H_2O)_z]^{x+} \rightarrow NiO_x(s) + Z\,H_2O\,(g) \quad (6)$$

After annealing, the NiO_x thin film shows as dense and compact, as shown in Figs. 2(b)–2(d). Moreover, NiO_x thin film's optical properties were also conducted by spectrophotometer at elevated temperature. Figure S1a (available online at stacks.iop.org/APEX/15/015504/mmedia) shows the UV–Vis absorbance spectrophotometer of the NiO_x thin film at 250 °C, 350 °C, 450 °C, and FTO showed no absorbance along the 400–1100 nm area that indicates almost all the light in the 400–1100 nm area was penetrated through the films. Only the 250 °C annealing temperature shows low absorbance at 400–1100 nm area. In Fig. S1b, all films exhibited a more than 50% transmittance value below 350 nm and dropped significantly on the band edge, indicating good film crystallinity. Furthermore, by calculating and plotting the absorbance data to transmittance, it is clearly seen that the bare FTO itself has absorbed the light less than 20%. At elevated temperatures, 350 °C and 450 °C show that the percentage transmittance of 350 °C and 450 °C are close to the FTO transmittance value. It indicates that NiO_x thin films at 350 °C and 450 °C have only slightly absorbed the light and demonstrates an insignificant transmittance value of 350 °C and 450 °C. On the other hand, at 250 °C, the annealing temperature showed no more than 70% in 400–1100 nm. This low transmittance is caused by carbon residue from incomplete combustion or oxidation reaction from the organic precursor. In Fig. S1c, the absorption coefficient (α) at elevated temperatures was also determined from absorbance or transmittance data using the derivation of the Lambert–Beer's equation. The absorption coefficient calculated using this equation shows NiO_x has a high absorption coefficient (α) of more than 10^5, indicating NiO_x can easily absorb the photons and is suitable as a p-type semiconductor. This value is also comparable with Ref. 32. Furthermore, in Fig. S1d, bandgap energy also can be determined by extrapolation of absorption coefficient data that is plotted into Tauc's equation ($\alpha h\nu = A(h\nu\text{-}E_g)^{1/2}$), where A is a constant and $h\nu$ is the incident photon energy. The bandgap energy of elevated temperature shows 3.31 eV for annealing temperatures of 250 °C, and 3.38 eV for annealing temperatures of 350 °C and 450 °C. In comparison, the NiO_x control shows high transmittance and has a bandgap of 3.20 eV. However, all of this bandgap energy was suitable to perovskite of 1.15 eV[33] as an active layer deposited on the NiO_x thin film. Figure S4 shows the optical properties of NiO_x thin films at elevated temperatures. The NiO_x thin film was characterized by XRD and XPS. The NiO_x XRD pattern was matched with NiO_x standard (ICDD #00–078–0643) at $2\theta = 37.29°$, 43.37°, and 62.96° as shown in Fig. 3(a). And confirmed by XPS spectra Ni(2p) in Fig. 3(b) and XPS spectra for O(1 s) Fig. 3(c). Figure 3(b) shows Ni($2p_{3/2}$) region that exhibits two peaks around 850 eV and 855 eV that indicates Ni^{3+} and Ni^{2+}, respectively. Moreover, in Ni($2p_{1/2}$), the region also shows two peaks representing Ni^{3+} and Ni^{2+} around 870 eV to 874 eV. This phenomenon indicates that the NiO_x thin film contains not only Ni^{2+} compounds but also Ni^{3+} compounds. Figure 3(c) shows O(1 s) spectra that show two peaks around 530 eV to 532 eV for octahedral bonding configuration, hydroxyl groups/adsorbed water, and a peak at 529 eV shows oxygen bonding with Ni^{2+}.[34] After obtaining the optimum condition for the synthesis of the NiO_x thin film, the next step was making inverted PSCs. Thus, it is crucial to find out the optimum thickness of NiO_x as an HTL to obtain the best performance devices. In order to control the thickness, NiO_x deposition was repeated several times. For the first deposition time, repetition of deposition has an approximate thickness of 23.20 nm with an average PCE of 5.49% and a maximum of 7.63%. The working device indicated that the FTO was covered by the NiO_x thin film even in a very thin layer. However, because there were some uncovered FTO areas by NiO_x, it can cause perovskite contact directly with the FTO and cause a short circuit. Moreover, even though NiO_x covered some FTO areas, the NiO_x layer was too thin, making the electron blockage ineffective. These conditions were causing the solar cells to have a low performance. The NiO_x thin film begins to cover the FTO surface completely when increasing repeat deposition completely from second to fourth deposition repetition. The performance was also enhanced, it is marked in increasing the J_{SC}, V_{OC}, and

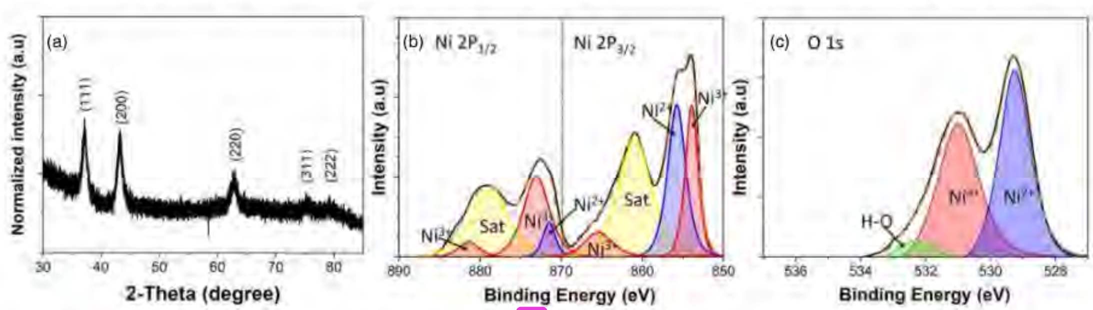

Fig. 3. (Color online) (a) XRD pattern of NiO_x thin film, and (b) XPS spectra of Ni (2p) and O (1 s) region of NiO_x thin film after annealing.

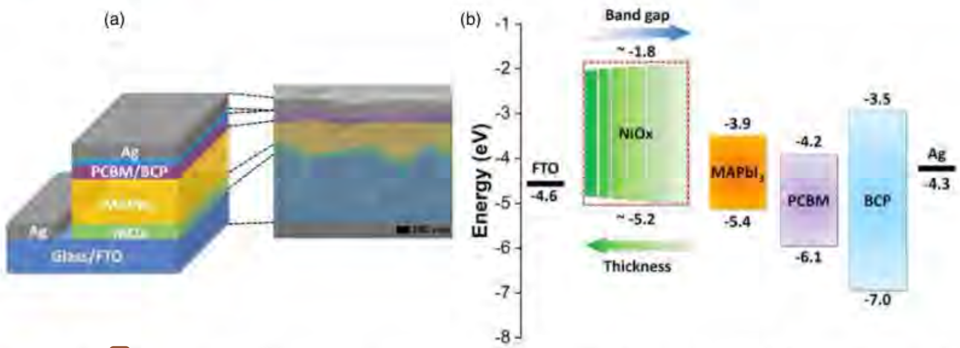

Fig. 4. (Color online) (a) Device structure of the inverted perovskite solar cells (PSCs), and (b) the energy band level diagram of the various layers in the PSCs.

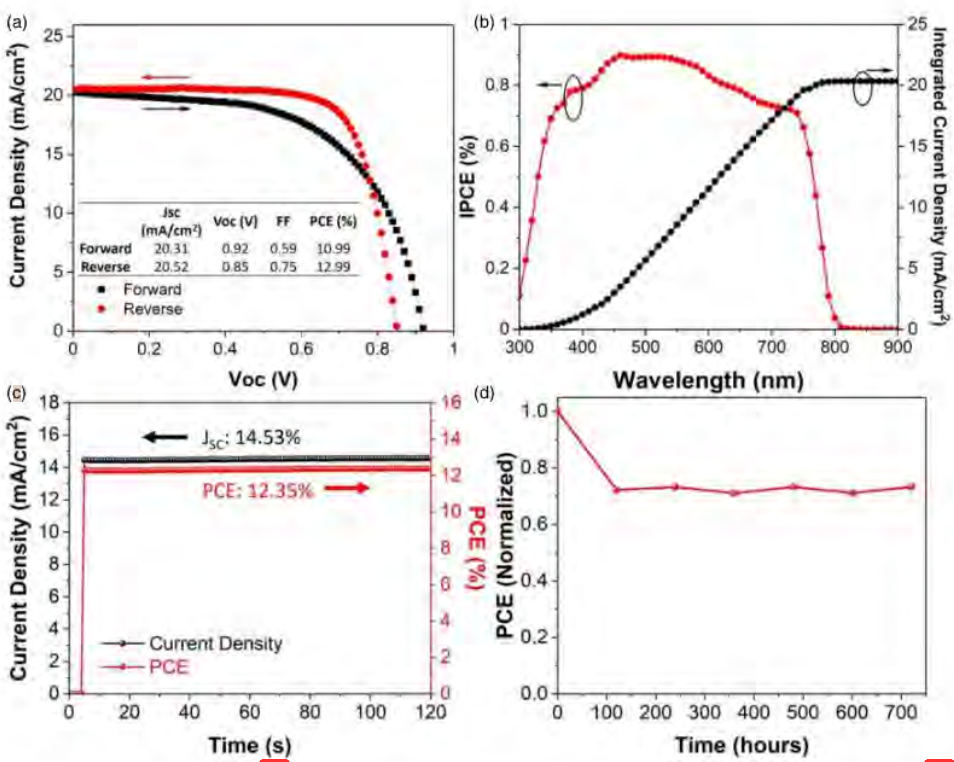

Fig. 5. (Color online) (a) J–V curves, (b) the IPCE spectrum of the best performing inverted PSCs using NiO_x powder with NiO_x reference. (c) steady-state efficiency, and (d) air stability of inverted PSCs using HTL from NiO_x thin films.

PCE values. At four times deposition repetition, the thickness was approximately 70.52 nm with J_{SC}, V_{OC}, FF, and PCE at a reverse scan direction of 20.52 mA cm^{-2}, 0.85 V, 0.74 12.99%, respectively. The FTO surface was well covered by the NiO_x thin film. Furthermore, repetition deposition for the fifth and sixth times exhibits a decreasing maximum PCE from 12.14% to 10.20%, respectively. The decrease of PCE was because of the increasing series resistance due to the increased thickness,[35] and the NiO_x thin film's thickness was higher than its Debye length, thus increasing its insulation properties. At some point, its electrical properties become insulators or bulk-like properties.[36] On the other hand, due to the high NiO_x absorption coefficient, increasing the thickness of NiO_x also reduces the light that passes through the NiO_x, and less light can be produced as current. Moreover, increasing the NiO_x thickness also shifted the bandgap of NiO_x that can slightly mismatch the bandgap value with the perovskite layer, as shown in Fig. 4. Moreover, Fig. 5(a) shows the optimum condition, with J_{SC}, V_{OC}, FF, and PCE at a reverse scan direction of 20.52 mA cm^{-2}, 0.85 V, 0.74, and 12.99%, respectively. Meanwhile, Fig. 5(b) shows the incident photon-to-electron conversion efficiency (IPCE) exhibits a relatively high quantum efficiency in the visible region and shows an integrated current density of 20.15 mA cm^{-2}, closely matching the measured J_{SC} values of 20.52 mA cm^{-2}. Moreover, in Fig. 5(c), the steady-state photocurrent output of NiO_x powder also exhibited stable performance as NiO_x reference for 160 s at the maximum V_{OC} of 0.85 V. In addition, we monitored the unencapsulated NiO_x powder-based device performance for 700 h to examine the device's stability. The devices were stored in a dry ambient environment with 30%–40% relative humidity as shown in Fig. 5(d).

In conclusion, the NiO_x thin film was successfully synthesized from NiO_x powder and applied as an HTL by a simple process using ethanol as the main solvent and nitric acid of less than 2% as the co-solvent, then applied as an HTL in inverted PSCs. The NiO_x thin film was deposited on FTO as a thin film by spin coating at 4000 rpm for 30 s and then annealing at 350 °C for 3 h under ambience temperature. The NiO_x thin film shows good optical properties and exhibits a PCE of 12.99% with J_{SC} of 20.52 mA cm^{-2}, V_{OC} of 0.85 V, and FF of 0.74. The thickness of NiO_x on inverted PSCs also exhibits an optimum condition at four times deposition repetition with a thickness of approximately 70.52 nm. This device also maintains efficiency around 70% of its initial efficiency.

Acknowledgments Thanks to The National University of Malaysia through the research grant support with code (LRGS/1/2019/UKM-UKM/6/1). This study was greatly supported by the Grant-in-Aid for Scientific Research Grant No. 20H02838 for financial support. The authors also extended their appreciation to The Taif University Researches Supporting Project No. (TURSP-2020/248), Taif University, Taif, Saudi Arabia. The authors also gratefully acknowledge the Ministry of Education and Culture of the Republic of Indonesia for the financial support as the BPPLN 2019 scholarship was granted to Ersan Y. Muslih.

ORCID IDs Md. Shahiduzzaman https://orcid.org/0000-0002-3092-7793 Md. Akhtaruzzaman https://orcid.org/0000-0002-7891-6321 Mohammad Ismail Hossain https://orcid.org/0000-0003-1290-9329 LiangLe Wang https://orcid.org/0000-0001-8386-0417 Jean-Michel Nunzi https://orcid.org/0000-0001-5490-4273

1) H. S. Kim et al., Sci. Rep. **2**, 1 (2012).
2) M. Shahiduzzaman, S. Fukaya, E. Y. Muslih, L. Wang, M. Nakano, M. Akhtaruzzaman, M. Karakawa, K. Takahashi, J. M. Nunzi, and T. Taima, Materials (Basel). **13**, 2207 (2020).
3) M. Shahiduzzaman et al., ACS Appl. Mater. Interfaces **13**, 21194 (2021).
4) M. Shahiduzzaman et al., Chem. Eng. J. **411**, 128461 (2021).
5) M. I. Hossain, A. M. Saleque, S. Ahmed, I. Saidjafarzoda, M. Shahiduzzaman, W. Qarony, D. Knipp, N. Biyikli, and Y. H. Tsang, Nano Energy **79**, 105400 (2021).
6) L. Wang, M. Shahiduzzaman, E. Y. Muslih, M. Nakano, M. Karakawa, K. Tomita, O. Lebel, J. M. Nunzi, and T. Taima, ACS Appl. Energy Mater. **4**, 12232 (2021).
7) S. Ye et al., J. Am. Chem. Soc. **139**, 7504 (2017).
8) N. Arora, M. I. Dar, A. Hinderhofer, N. Pellet, F. Schreiber, S. M. Zakeeruddin, and M. Grätzel, Science **358**, 768 (2017).
9) J. He, E. Bi, W. Tang, Y. Wang, Z. Zhou, X. Yang, H. Chen, and L. Han, Sol. RRL **2**, 1 (2018).
10) M. I. Hossain et al., Small Methods **4**, 2000454 (2020).
11) A. K. M. Hasan et al., Results Phys. **17**, 103122 (2020).
12) A. Venter and J. R. Botha, S. Afr. J. Sci. **107**, 268 (2011).
13) M. D. Irwin, D. B. Buchholz, A. W. Hains, R. P. H. Chang, and T. J. Marks, Proc. Natl. Acad. Sci. U. S. A. **105**, 2783 (2008).
14) M. L. Grilli, F. Menchini, T. Dikonimos, P. Nunziante, L. Pilloni, M. Yilmaz, A. Piegari, and A. Mittiga, Semicond. Sci. Technol. **31**, 55016 (2016).
15) F. Ma, Y. Zhao, J. Li, X. Zhang, H. Gu, and J. You, J. Energy Chem. **52**, 393 (2020).
16) W. Chen, F. Z. Liu, X. Y. Feng, A. B. Djurišić, W. K. Chan, and Z. B. He, Adv. Energy Mater. **7**, 1700722 (2017).
17) W. J. Scheideler, N. Rolston, O. Zhao, J. Zhang, and R. H. Dauskardt, Adv. Energy Mater. **9**, 1803600 (2019).
18) M. Najafi et al., Small **14**, 1702775 (2018).
19) Z. Zhu, Y. Bai, X. Liu, C. C. Chueh, S. Yang, and A. K. Y. Jen, Adv. Mater. **28**, 6478 (2016).
20) S. Xiao, Y. Bai, X. Meng, T. Zhang, H. Chen, X. Zheng, C. Hu, Y. Qu, and S. Yang, Adv. Funct. Mater. **27**, 1604944 (2017).
21) P. Zhou, B. Li, Z. Fang, W. Zhou, M. Zhang, W. Hu, T. Chen, Z. Xiao, and S. Yang, Sol. RRL **3**, 1970111 (2019).
22) K. D. A. Kumar, S. Valanarasu, A. Kathalingam, V. Ganesh, M. Shkir, and S. AlFaify, Appl. Phys. A Mater. Sci. Process. **123**, 1 (2017).
23) K. X. Steirer et al., J. Mater. Chem. A **3**, 10949 (2015).
24) A. Cho, H. Song, J. Gwak, Y.-J. Eo, J. H. Yun, K. Yoon, and S. Ahn, J. Mater. Chem. A **2**, 5087 (2014).
25) M. Aminuzzaman, C. Y. Chong, W. S. Goh, Y. K. Phang, T. Lai-Hock, S. Y. Chee, M. Akhtaruzzaman, S. Ogawa, and A. Watanabe, J. Clust. Sci. **32**, 949 (2021).
26) X. Lian, J. Chen, S. Shan, G. Wu, and H. Chen, ACS Appl. Mater. Interfaces **12**, 46340 (2020).
27) D. Thakur, S. E. Chiang, M. H. Yang, J. S. Wang, and S. H. Chang, Sol. Energy Mater. Sol. Cells **235**, 111454 (2022).
28) J. Zhang, J. Long, Z. Huang, J. Yang, X. Li, R. Dai, W. Sheng, L. Tan, and Y. Chen, Chem. Eng. J. **426**, 131357 (2021).
29) N. Tiwari, H. Arianita Dewi, E. Erdenebileg, R. Narayan Chauhan, N. Mathews, S. Mhaisalkar, and A. Bruno, Sol. RRL. 2100700 (2021).
30) R. R. T. Marinho, M. M. Walz, V. Ekholm, G. Öhrwall, O. Björneholm, and A. N. De Brito, J. Phys. Chem. B **121**, 7916 (2017).
31) E. A. Cochran, K. N. Woods, D. W. Johnson, C. J. Page, and S. W. Boettcher, J. Mater. Chem. A **7**, 24124 (2019).
32) A. A. Al-Ghamdi, W. E. Mahmoud, S. J. Yaghmour, and F. M. Al-Marzouki, J. Alloys Compd. **486**, 9 (2009).
33) M. Caputo et al., Sci. Rep. **9**, 15159 (2019).
34) S. S. Mali, H. Kim, S. E. Shim, and C. K. Hong, Nanoscale **8**, 19189 (2016).
35) X. Yin et al., ACS Appl. Mater. Interfaces **9**, 2439 (2017).
36) S. Seo, I. J. Park, M. Kim, S. Lee, C. Bae, H. S. Jung, N. G. Park, J. Y. Kim, and H. Shin, Nanoscale **8**, 11403 (2016).

Reproducible perovskite solar cells using a simple solvent-mediated sol−gel synthesized NiOx hole transport layer

ORIGINALITY REPORT

12%	8%	12%	4%
SIMILARITY INDEX	INTERNET SOURCES	PUBLICATIONS	STUDENT PAPERS

PRIMARY SOURCES

1	Ersan Y. Muslih, Khan Sobayel Bin Rafiq, Mohammad Ismail Hossain, Shahiduzzaman et al. "Growth and Reaction Mechanism of Solution-processed Cu2ZnSnSe4 Thin Films for Realising Efficient Photovoltaic Applications", Journal of Alloys and Compounds, 2021 Publication	2%
2	Mohammad Ismail Hossain, Md. Shahiduzzaman, Safayet Ahmed, Md. Rashedul Huqe et al. "Near field control for enhanced photovoltaic performance and photostability in perovskite solar cells", Nano Energy, 2021 Publication	1%
3	doaj.org Internet Source	1%
4	Yunxiang Wang, Jihua Zhang, Yanhua Wu, Zichuan Yi, Feng Chi, Honghang Wang, Wanshu Li, Yan Zhang, Xiaowen Zhang, Liming	1%

Liu. "Solution-processed bathocuproine cathode buffer layer towards efficient planar heterojunction perovskite solar cells", Semiconductor Science and Technology, 2019
Publication

5	www.pubfacts.com Internet Source	1%
6	pubs.acs.org Internet Source	1%
7	Xingxing Wan, Yanan Jiang, Zhiwen Qiu, Hailiang Zhang, Xiaomeng Zhu, Iqbal Sikandar, xiaobin liu, Xin Chen, Bingqiang Cao. "Zinc as new dopant for NiOx based planar perovskite solar cells with stable efficiency near 20%", ACS Applied Energy Materials, 2018 Publication	1%
8	Bairu Li, Jieming Zhen, Yangyang Wan, Xunyong Lei et al. "Steering the electron transport properties of pyridine-functionalized fullerene derivatives in inverted perovskite solar cells: the nitrogen site matters", Journal of Materials Chemistry A, 2020 Publication	1%
9	Jiangshan Feng, Zhou Yang, Dong Yang, Xiaodong Ren, Xuejie Zhu, Zhiwen Jin, Wei Zi, Qingbo Wei, Shengzhong (Frank) Liu. "E-beam evaporated Nb 2 O 5 as an effective electron transport layer for large flexible perovskite	1%

solar cells", Nano Energy, 2017
Publication

10	Chen Hu, Yang Bai, Shuang Xiao, Teng Zhang, Xiangyue Meng, Wai Kit Ng, Yinglong Yang, Kam Sing Wong, Haining Chen, Shihe Yang. "Tuning the A-site cation composition of FA perovskites for efficient and stable NiO-based p–i–n perovskite solar cells", J. Mater. Chem. A, 2017 Publication	1 %
11	Submitted to Universitas Brawijaya Student Paper	1 %
12	Namyoung Ahn, Dae-Yong Son, In-Hyuk Jang, Seong Min Kang, Mansoo Choi, Nam-Gyu Park. "Highly Reproducible Perovskite Solar Cells with Average Efficiency of 18.3% and Best Efficiency of 19.7% Fabricated via Lewis Base Adduct of Lead(II) Iodide", Journal of the American Chemical Society, 2015 Publication	<1 %
13	Xingyue Liu, Zhiyong Liu, Bo Sun, Xianhua Tan, Haibo Ye, Yuxue Tu, Tielin Shi, Zirong Tang, Guanglan Liao. "17.46% efficient and highly stable carbon-based planar perovskite solar cells employing Ni-doped rutile TiO 2 as electron transport layer", Nano Energy, 2018 Publication	<1 %

14	T. Selvan Ponmudi, Ching-Wei Lee, Chien-Chih Lai, Chih-Hung Tsai. "Comparative study on the effect of annealing temperature on sol–gel-derived nickel oxide thin film as hole transport layers for inverted perovskite solar cells", Journal of Materials Science: Materials in Electronics, 2021 Publication	<1 %
15	dokumen.pub Internet Source	<1 %
16	erj.ersjournals.com Internet Source	<1 %
17	worldwidescience.org Internet Source	<1 %

Exclude quotes	On	Exclude matches	< 10 words
Exclude bibliography	On		

Reproducible perovskite solar cells using a simple solvent-mediated sol−gel synthesized NiOx hole transport layer

GRADEMARK REPORT

FINAL GRADE	GENERAL COMMENTS
/0	

PAGE 1

PAGE 2

PAGE 3

PAGE 4

PAGE 5

PAGE 6

Applied Physics
Express

LETTER

Reproducible perovskite solar cells using a simple solvent-mediated sol−gel synthesized NiO_x hole transport layer

Applied Physics Express **15**, 015504 (2022) **LETTER**
https://doi.org/10.35848/1882-0786/ac435d

Reproducible perovskite solar cells using a simple solvent-mediated sol–gel synthesized NiO_x hole transport layer

Ersan Y. Muslih[1,2], Md. Shahiduzzaman[3*], Md. Akhtaruzzaman[4*], Mohammad Ismail Hossain[5], LiangLe Wang[6], Hend I. Alkhammash[7], Sami S. Alharthi[8], Masahiro Nakano[1], Makoto Karakawa[1,3], Mohammod Aminuzzaman[9,10], Lai-Hock Tey[9], Kamaruzzaman Sopian[4], Jean-Michel Nunzi[3], and Tetsuya Taima[1,3,6*]

[1]Graduate School of Natural Science and Technology, Kanazawa University, Kakuma, Kanazawa 920–1292, Japan
[2]Mechanical Engineering Department, Faculty of Industrial Technology, Trisakti University, Jakarta 11440, Indonesia
[3]Nanomaterials Research Institute, Kanazawa University, Kakuma, Kanazawa 920–1192, Japan
[4]Solar Energy Research Institute (SERI), Universiti Kebangsaan Malaysia (UKM), 43600 Bangi, Selangor, Malaysia
[5]Department of Electrical and Computer Engineering, University of California, Davis, 1 Shields Avenue, Davis, CA 95616, United States of America
[6]Graduate School of Frontier Science Initiative, Kanazawa University, Kakuma, Kanazawa 920–1192, Japan
[7]Department of Electrical Engineering, College of Engineering, Taif University, P.O.Box 11099, Taif 21944, Saudi Arabia
[8]Department of Physics, College of Science, Taif University, PO Box 11099, Taif 21944, Saudi Arabia
[9]Department of Chemical Science, Faculty of Science, Universiti Tunku Abdul Rahman, Perak Campus, Jalan Universiti, Bandar Barat, 31900 Kampar, Perak D. R., Malaysia
[10]Centre for Photonics and Advanced Materials Research (CPAMR), Universiti Tunku Abdul Rahman, Jalan Sungai Long, Bandar Sungai Long, 43000 Kajang, Selangor, Malaysia

*E-mail: shahiduzzaman@se.kanazawa-u.ac.jp; akhtar@ukm.edu.my; taima@se.kanazawa-u.ac.jp

Received November 29, 2021; revised December 8, 2021; accepted December 14, 2021; published online January 6, 2022

A nickel oxide (NiO_x) hole transport layer was made from nickel oxide powder by a simple process and non-stabilizer or chelating agent. We used ethanol as the main solvent and less than 2% nitric acid as the co-solvent. The formation reaction mechanism of the NiO_x thin film was also studied. Perovskite solar cells (PSCs) with an optimum thickness of 70 nm exhibited a power conversion efficiency as high as 12.99%, which is superior to those of PSCs with their counterparts. The moisture stability of NiO_x-based devices (non-encapsulated) remained above 70% of their initial output after 700 h storage at ambient conditions.

Supplementary material for this article is available online

Since being discovered by Park in 2012,[1)] organic–inorganic halide perovskite solar cells (PSCs) have triggered rapid development and much attention because of their potential to more developed relatively low-cost processing, up-scale applicable, and having two well-known conventional n-i-p and inverted p-i-n structures.[2–4)] Both structure-based devices use organic materials such as 2,2′,7,7′-tetrakis[*N*,*N*-di(4-methoxyphenyl)amino]−9,9′-spirobifluorene (spiro-OMeTAD) and polymer poly[bis(4-phenyl)(2,4,6-trimethylphenyl)amine] (PTAA) as the hole transport layers (HTLs), which are high-cost and low-stability.[5,6)] Thus, inorganic HTL materials attract more attention to replace the organic HTLs due to superior hole-mobility and outstanding stability. Inorganic p-type semiconductor materials such as CuI, CuSCN, and NiO_x have been developed as HTL in PSCs to solve these problems.[7–11)] Among inorganic HTL, nickel oxide (NiO_x) is the most prominent and attractive HTLs mentioned above because it is relatively inert and intrinsically p-type with a wide bandgap (3.15–4.3 eV).[9–14)] Typically, NiO_x thin film is made by sol-gel from nickel salts such as nickel acetate, nickel nitrate, and nickel acetylacetonate.[9,15–21)] However, those sol-gel techniques are time-consuming and require a stabilizer or complexing agents such as ethanolamine that can have high sheet resistance, resistivity, low conductivity, and low carrier concentration.[21–24)] Previously, Akhtaruzzaman and colleagues[25)] produced NiO_x powder particles with a diameter of 100 nm or bigger by green synthesis. In terms of PSC application, these bigger NiO_x particles cannot be a suitable candidate as the solely HTL because inadequate surface coverage and electron blockage leads to perovskite penetration into FTO-substrate and makes a short circuit. Therefore, it is important to make NiO_x particles as a compact and dense thin film for HTL application in PSCs, which has not been studied in-depth and used as an HTL solely for PSCs applications.

In this work, a compact NiO_x thin film has been successfully synthesized from nickel oxide powder using a simple solution mixture between low content nitric acid as a co-solvent and ethanol as the main solvent and applied as the HTL for inverted PSCs. The inverted p-i-n structure-based device was chosen due to relatively low process temperature and is widely open to making a tandem solar cell with conventional low-bandgap p-type photovoltaics.[26–29)] The reaction mechanism of the formation NiO_x thin film was also investigated. NiO_x thin films showed a favorable energy level with perovskite film, most importantly low-cost and environment-friendly synthesis capabilities. The HTL exhibits a high crystallinity, suitable optical properties, good performance, and good stability of inverted PSCs.

Metal oxides are immiscible in water or other solvents with similar to water properties such as alcohol. Thus, to solve NiO_x powder, nitric acid was added and followed with heat treatment at 85° for about 10 min. This treatment can ionize the NiO_x into Ni^{2+} and react with NO_3^- and water molecules to form complex compounds that dissolve in ethanol. Besides being the main solvent, ethanol also reduces surface tension so that the solution can stick to the substrate more. Figure 1 shows the few steps of the NiO_x thin-film making process from NiO_x powder. In the solving process, the reaction would only happen if assisted by heating and made an azeotrope compound with nitrate and water molecules. This process was marked by color changing from a black powder into a green solution. NiO_x powder was dissolved in nitric acid and water molecules to make some ionic complex compounds. At this point, the nickel complex molecule was surrounded by

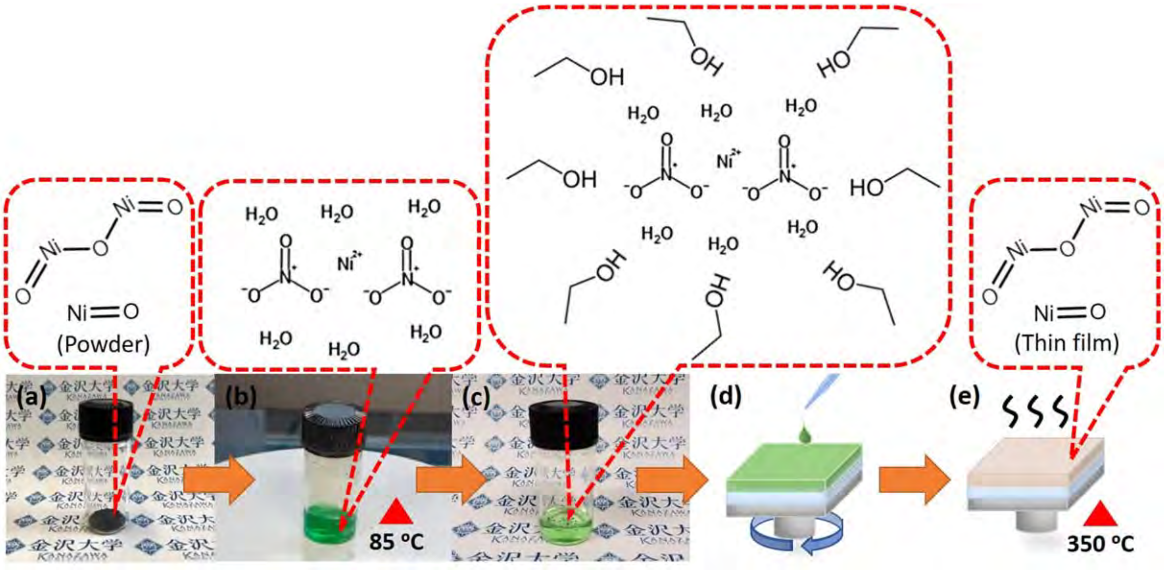

Fig. 1. (Color online) (a) NiO_x powder (b) NiO_x powder dissolving process with nitric acid and heat, (c) appearance of NiO_x solution after diluted with ethanol, (d) illustration of NiO_x solution deposited on FTO glass by spin-coating, (e) annealing illustration of NiO_x thin film.

ethanol molecules as its solvent. Besides solvation interaction, there is also hydrogen bonding between water and ethanol.[30] This phenomenon was easily recognized when the color was changed and easily dissolved in ethanol and recorded by a UV–vis spectrophotometry peak shift from 394 nm to 399 nm, as shown in Fig. 2(a). Furthermore, this solution was deposited on FTO and followed by annealing to obtain NiO_x thin films. Finally, nickel ion underwent an oxidation reaction or condensation and formed NiO_x. These reactions were matched with Boetcher et al.,[31] which explains the reactions of metal-oxide synthesis from metal-nitrate in detail. However, the reactions in this research were divided into three stages, the first is the dissolution reaction, the second is the nitrate thermal decomposition, and the last stage is the metal oxide formation stage. Overall, the NiO_x thin film synthesis was described as using the following reactions:

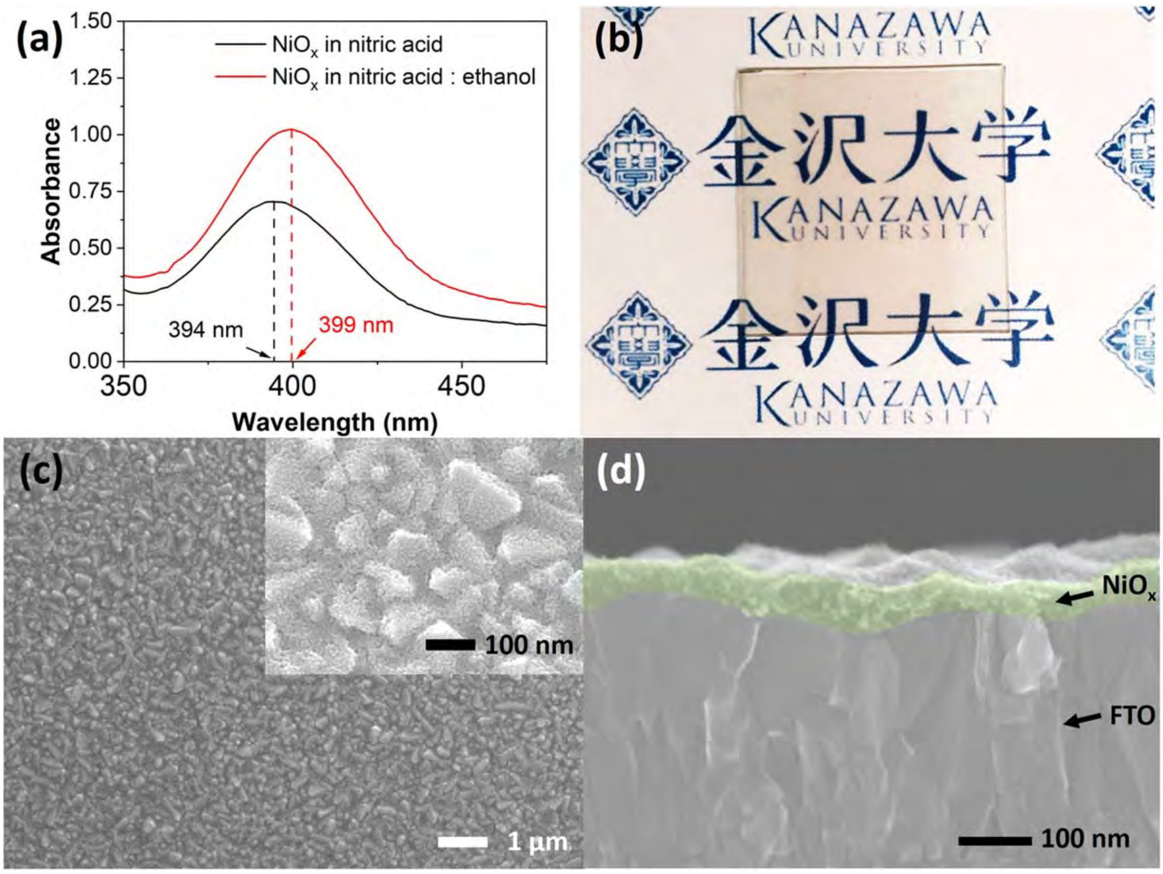

Fig. 2. (Color online) (a) The UV–vis spectra for NiO_x in nitric acid and nitric acid with ethanol, (b) NiO_x thin film appearance after annealing, (c) top view SEM image of NiO_x thin film, and (d) cross-sectional SEM image of NiO_x thin film on FTO.

Dissolution Reaction:

$$NiO_x(s) + 2\,HNO_3\,(aq) + Z\,H_2O(aq) \rightarrow Ni(NO_3)_x.ZH_2O\,(aq) \quad (1)$$

$$Ni(NO_3)_x.ZH_2O\,(aq) \rightarrow [Ni(H_2O)_z]^{x+}(aq) + Z\,HNO_3(aq) \quad (2)$$

Nitrate Thermal Decomposition:

$$Ni(NO_3)_x.ZH_2O\,(aq) \rightarrow Ni(OH)_x(aq) + X\,NO_2(g) + Z\,H_2O\,(g) \quad (3)$$

$$4\,HNO_3(aq) \rightarrow 4\,NO_2(g) + O_2(g) + 2\,H_2O\,(g) \quad (4)$$

Metal Oxide Formation:

$$Ni(OH)_x(aq) \rightarrow NiO_x(s) + Z\,H_2O\,(g) \quad (5)$$

$$[Ni(H_2O)_z]^{x+} \rightarrow NiO_x(s) + Z\,H_2O\,(g) \quad (6)$$

After annealing, the NiO_x thin film shows as dense and compact, as shown in Figs. 2(b)–2(d). Moreover, NiO_x thin film's optical properties were also conducted by spectrophotometer at elevated temperature. Figure S1a (available online at stacks.iop.org/APEX/15/015504/mmedia) shows the UV–Vis absorbance spectrophotometer of the NiO_x thin film at 250 °C, 350 °C, 450 °C, and FTO showed no absorbance along the 400–1100 nm area that indicates almost all the light in the 400–1100 nm area was penetrated through the films. Only the 250 °C annealing temperature shows low absorbance at 400–1100 nm area. In Fig. S1b, all films exhibited a more than 50% transmittance value below 350 nm and dropped significantly on the band edge, indicating good film crystallinity. Furthermore, by calculating and plotting the absorbance data to transmittance, it is clearly seen that the bare FTO itself has absorbed the light less than 20%. At elevated temperatures, 350 °C and 450 °C show that the percentage transmittance of 350 °C and 450 °C are close to the FTO transmittance value. It indicates that NiO_x thin films at 350 °C and 450 °C have only slightly absorbed the light and demonstrates an insignificant transmittance value of 350 °C and 450 °C. On the other hand, at 250 °C, the annealing temperature showed no more than 70% in 400–1100 nm. This low transmittance is caused by carbon residue from incomplete combustion or oxidation reaction from the organic precursor. In Fig. S1c, the absorption coefficient (α) at elevated temperatures was also determined from absorbance or transmittance data using the derivation of the Lambert–Beer's equation. The absorption coefficient calculated using this equation shows NiO_x has a high absorption coefficient (α) of more than 10^5, indicating NiO_x can easily absorb the photons and is suitable as a p-type semiconductor. This value is also comparable with Ref. 32. Furthermore, in Fig. S1d, bandgap energy also can be determined by extrapolation of absorption coefficient data that is plotted into Tauc's equation ($\alpha h\nu = A(h\nu\text{-}E_g)^{1/2}$), where A is a constant and $h\nu$ is the incident photon energy. The bandgap energy of elevated temperature shows 3.31 eV for annealing temperatures of 250 °C, and 3.38 eV for annealing temperatures of 350 °C and 450 °C. In comparison, the NiO_x control shows high transmittance and has a bandgap of 3.20 eV. However, all of this bandgap energy was suitable to perovskite of 1.15 eV[33] as an active layer deposited on the NiO_x thin film. Figure S4 shows the optical properties of NiO_x thin films at elevated temperatures. The NiO_x thin film was characterized by XRD and XPS. The NiO_x XRD pattern was matched with NiO_x standard (ICDD #00–078–0643) at $2\theta = 37.29°$, 43.37°, and 62.96° as shown in Fig. 3(a). And confirmed by XPS spectra Ni(2p) in Fig. 3(b) and XPS spectra for O(1 s) Fig. 3(c). Figure 3(b) shows $Ni(2p_{3/2})$ region that exhibits two peaks around 850 eV and 855 eV that indicates Ni^{3+} and Ni^{2+}, respectively. Moreover, in $Ni(2p_{1/2})$, the region also shows two peaks representing Ni^{3+} and Ni^{2+} around 870 eV to 874 eV. This phenomenon indicates that the NiO_x thin film contains not only Ni^{2+} compounds but also Ni^{3+} compounds. Figure 3(c) shows O(1 s) spectra that show two peaks around 530 eV to 532 eV for octahedral bonding configuration, hydroxyl groups/adsorbed water, and a peak at 529 eV shows oxygen bonding with Ni^{2+}.[34] After obtaining the optimum condition for the synthesis of the NiO_x thin film, the next step was making inverted PSCs. Thus, it is crucial to find out the optimum thickness of NiO_x as an HTL to obtain the best performance devices. In order to control the thickness, NiO_x deposition was repeated several times. For the first deposition time, repetition of deposition has an approximate thickness of 23.20 nm with an average PCE of 5.49% and a maximum of 7.63%. The working device indicated that the FTO was covered by the NiO_x thin film even in a very thin layer. However, because there were some uncovered FTO areas by NiO_x, it can cause perovskite contact directly with the FTO and cause a short circuit. Moreover, even though NiO_x covered some FTO areas, the NiO_x layer was too thin, making the electron blockage ineffective. These conditions were causing the solar cells to have a low performance. The NiO_x thin film begins to cover the FTO surface completely when increasing repeat deposition completely from second to fourth deposition repetition. The performance was also enhanced, it is marked in increasing the J_{SC}, V_{OC}, and

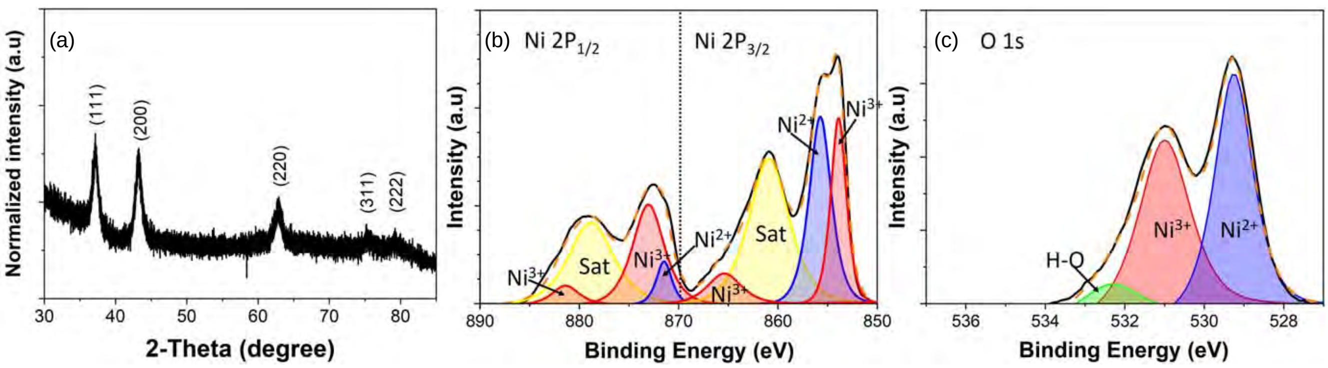

Fig. 3. (Color online) (a) XRD pattern of NiO_x thin film, and (b) XPS spectra of Ni (2p) and O (1 s) region of NiO_x thin film after annealing.

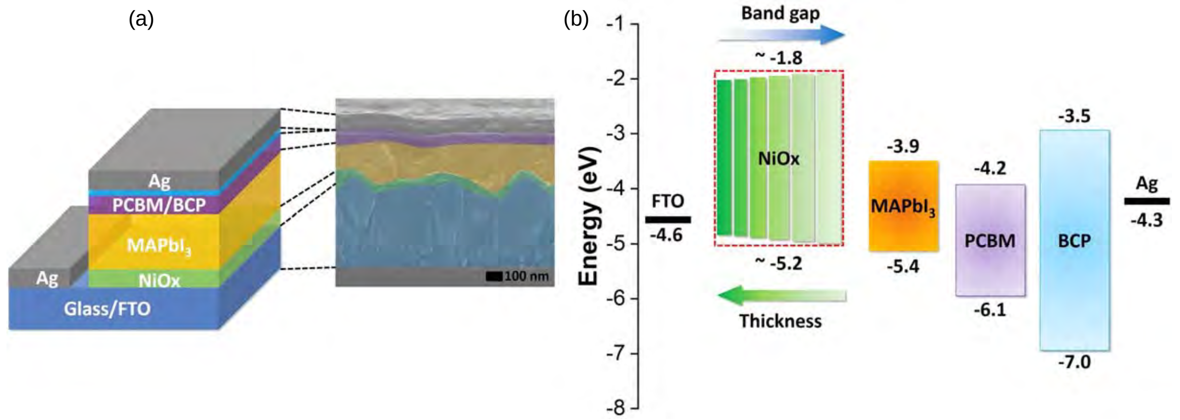

Fig. 4. (Color online) (a) Device structure of the inverted perovskite solar cells (PSCs), and (b) the energy band level diagram of the various layers in the PSCs.

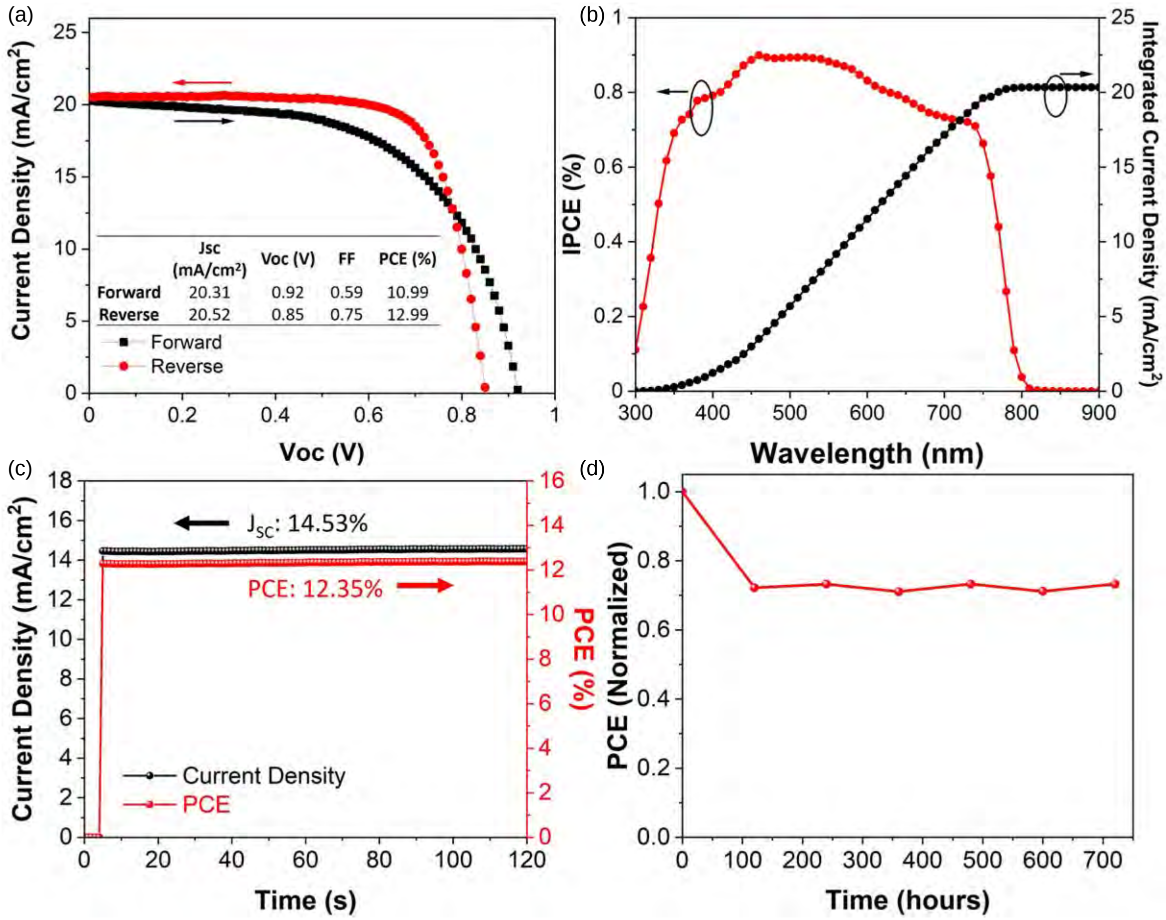

Fig. 5. (Color online) (a) *J–V* curves, (b) the IPCE spectrum of the best performing inverted PSCs using NiO_x powder with NiO_x reference. (c) steady-state efficiency, and (d) air stability of inverted PSCs using HTL from NiO_x thin films.

PCE values. At four times deposition repetition, the thickness was approximately 70.52 nm with J_{SC}, V_{OC}, FF, and PCE at a reverse scan direction of 20.52 mA cm^{-2}, 0.85 V, 0.74 12.99%, respectively. The FTO surface was well covered by the NiO_x thin film. Furthermore, repetition deposition for the fifth and sixth times exhibits a decreasing maximum PCE from 12.14% to 10.20%, respectively. The decrease of PCE was because of the increasing series resistance due to the increased thickness,[35] and the NiO_x thin film's thickness was higher than its Debye length, thus increasing its insulation properties. At some point, its electrical properties become insulators or bulk-like properties.[36] On the other hand, due to the high NiO_x absorption coefficient, increasing the thickness of NiO_x also reduces the light that passes through the NiO_x, and less light can be produced as current. Moreover, increasing the NiO_x thickness also shifted the bandgap of NiO_x that can slightly mismatch the bandgap value with the perovskite layer, as shown in Fig. 4. Moreover, Fig. 5(a) shows the optimum condition, with J_{SC}, V_{OC}, FF, and PCE at a reverse scan direction of 20.52 mA cm^{-2}, 0.85 V, 0.74, and 12.99%, respectively. Meanwhile, Fig. 5(b) shows the incident photon-to-electron conversion efficiency (IPCE) exhibits a relatively high quantum efficiency in the visible region and shows an integrated current density of 20.15 mA cm^{-2}, closely matching the measured J_{SC} values of 20.52 mA cm^{-2}. Moreover, in Fig. 5(c), the steady-state photocurrent output of NiO_x powder also exhibited stable performance as NiO_x reference for 160 s at the maximum V_{OC} of 0.85 V. In addition, we monitored the unencapsulated NiO_x powder-based device performance for 700 h to examine the device's stability. The devices were stored in a dry ambient environment with 30%–40% relative humidity as shown in Fig. 5(d).

In conclusion, the NiO_x thin film was successfully synthesized from NiO_x powder and applied as an HTL by a simple process using ethanol as the main solvent and nitric acid of less than 2% as the co-solvent, then applied as an HTL in inverted PSCs. The NiO_x thin film was deposited on FTO as a thin film by spin coating at 4000 rpm for 30 s and then annealing at 350 °C for 3 h under ambience temperature. The NiO_x thin film shows good optical properties and exhibits a PCE of 12.99% with J_{SC} of 20.52 mA cm^{-2}, V_{OC} of 0.85 V, and FF of 0.74. The thickness of NiO_x on inverted PSCs also exhibits an optimum condition at four times deposition repetition with a thickness of approximately 70.52 nm. This device also maintains efficiency around 70% of its initial efficiency.

Acknowledgments Thanks to The National University of Malaysia through the research grant support with code (LRGS/1/2019/UKM-UKM/6/1). This study was greatly supported by the Grant-in-Aid for Scientific Research Grant No. 20H02838 for financial support. The authors also extended their appreciation to The Taif University Researches Supporting Project No. (TURSP-2020/248), Taif University, Taif, Saudi Arabia. The authors also gratefully acknowledge the Ministry of Education and Culture of the Republic of Indonesia for the financial support as the BPPLN 2019 scholarship was granted to Ersan Y. Muslih.

ORCID iDs Md. Shahiduzzaman https://orcid.org/0000-0002-3092-7793 Md. Akhtaruzzaman https://orcid.org/0000-0002-7891-6321 Mohammad Ismail Hossain https://orcid.org/0000-0003-1290-9329 LiangLe Wang https://orcid.org/0000-0001-8386-0417 Jean-Michel Nunzi https://orcid.org/0000-0001-5490-4273

1) H. S. Kim et al., Sci. Rep. **2**, 1 (2012).
2) M. Shahiduzzaman, S. Fukaya, E. Y. Muslih, L. Wang, M. Nakano, M. Akhtaruzzaman, M. Karakawa, K. Takahashi, J. M. Nunzi, and T. Taima, Materials (Basel). **13**, 2207 (2020).
3) M. Shahiduzzaman et al., ACS Appl. Mater. Interfaces **13**, 21194 (2021).
4) M. Shahiduzzaman et al., Chem. Eng. J. **411**, 128461 (2021).
5) M. I. Hossain, A. M. Saleque, S. Ahmed, I. Saidjafarzoda, M. Shahiduzzaman, W. Qarony, D. Knipp, N. Biyikli, and Y. H. Tsang, Nano Energy **79**, 105400 (2021).
6) L. Wang, M. Shahiduzzaman, E. Y. Muslih, M. Nakano, M. Karakawa, K. Tomita, O. Lebel, J. M. Nunzi, and T. Taima, ACS Appl. Energy Mater. **4**, 12232 (2021).
7) S. Ye et al., J. Am. Chem. Soc. **139**, 7504 (2017).
8) N. Arora, M. I. Dar, A. Hinderhofer, N. Pellet, F. Schreiber, S. M. Zakeeruddin, and M. Grätzel, Science **358**, 768 (2017).
9) J. He, E. Bi, W. Tang, Y. Wang, Z. Zhou, X. Yang, H. Chen, and L. Han, Sol. RRL **2**, 1 (2018).
10) M. I. Hossain et al., Small Methods **4**, 2000454 (2020).
11) A. K. M. Hasan et al., Results Phys. **17**, 103122 (2020).
12) A. Venter and J. R. Botha, S. Afr. J. Sci. **107**, 268 (2011).
13) M. D. Irwin, D. B. Buchholz, A. W. Hains, R. P. H. Chang, and T. J. Marks, Proc. Natl. Acad. Sci. U. S. A. **105**, 2783 (2008).
14) M. L. Grilli, F. Menchini, T. Dikonimos, P. Nunziante, L. Pilloni, M. Yilmaz, A. Piegari, and A. Mittiga, Semicond. Sci. Technol. **31**, 55016 (2016).
15) F. Ma, Y. Zhao, J. Li, X. Zhang, H. Gu, and J. You, J. Energy Chem. **52**, 393 (2020).
16) W. Chen, F. Z. Liu, X. Y. Feng, A. B. Djurišić, W. K. Chan, and Z. B. He, Adv. Energy Mater. **7**, 1700722 (2017).
17) W. J. Scheideler, N. Rolston, O. Zhao, J. Zhang, and R. H. Dauskardt, Adv. Energy Mater. **9**, 1803600 (2019).
18) M. Najafi et al., Small **14**, 1702775 (2018).
19) Z. Zhu, Y. Bai, X. Liu, C. C. Chueh, S. Yang, and A. K. Y. Jen, Adv. Mater. **28**, 6478 (2016).
20) S. Xiao, Y. Bai, X. Meng, T. Zhang, H. Chen, X. Zheng, C. Hu, Y. Qu, and S. Yang, Adv. Funct. Mater. **27**, 1604944 (2017).
21) P. Zhou, B. Li, Z. Fang, W. Zhou, M. Zhang, W. Hu, T. Chen, Z. Xiao, and S. Yang, Sol. RRL **3**, 1970111 (2019).
22) K. D. A. Kumar, S. Valanarasu, A. Kathalingam, V. Ganesh, M. Shkir, and S. AlFaify, Appl. Phys. A Mater. Sci. Process. **123**, 1 (2017).
23) K. X. Steirer et al., J. Mater. Chem. A **3**, 10949 (2015).
24) A. Cho, H. Song, J. Gwak, Y.-J. Eo, J. H. Yun, K. Yoon, and S. Ahn, J. Mater. Chem. A **2**, 5087 (2014).
25) M. Aminuzzaman, C. Y. Chong, W. S. Goh, Y. K. Phang, T. Lai-Hock, S. Y. Chee, M. Akhtaruzzaman, S. Ogawa, and A. Watanabe, J. Clust. Sci. **32**, 949 (2021).
26) X. Lian, J. Chen, S. Shan, G. Wu, and H. Chen, ACS Appl. Mater. Interfaces **12**, 46340 (2020).
27) D. Thakur, S. E. Chiang, M. H. Yang, J. S. Wang, and S. H. Chang, Sol. Energy Mater. Sol. Cells **235**, 111454 (2022).
28) J. Zhang, J. Long, Z. Huang, J. Yang, X. Li, R. Dai, W. Sheng, L. Tan, and Y. Chen, Chem. Eng. J. **426**, 131357 (2021).
29) N. Tiwari, H. Arianita Dewi, E. Erdenebileg, R. Narayan Chauhan, N. Mathews, S. Mhaisalkar, and A. Bruno, Sol. RRL, 2100700 (2021).
30) R. R. T. Marinho, M. M. Walz, V. Ekholm, G. Öhrwall, O. Björneholm, and A. N. De Brito, J. Phys. Chem. B **121**, 7916 (2017).
31) E. A. Cochran, K. N. Woods, D. W. Johnson, C. J. Page, and S. W. Boettcher, J. Mater. Chem. A **7**, 24124 (2019).
32) A. A. Al-Ghamdi, W. E. Mahmoud, S. J. Yaghmour, and F. M. Al-Marzouki, J. Alloys Compd. **486**, 9 (2009).
33) M. Caputo et al., Sci. Rep. **9**, 15159 (2019).
34) S. S. Mali, H. Kim, S. E. Shim, and C. K. Hong, Nanoscale **8**, 19189 (2016).
35) X. Yin et al., ACS Appl. Mater. Interfaces **9**, 2439 (2017).
36) S. Seo, I. J. Park, M. Kim, S. Lee, C. Bae, H. S. Jung, N. G. Park, J. Y. Kim, and H. Shin, Nanoscale **8**, 11403 (2016).